INTERNATIONAL JOURNAL OF
RADIATION ONCOLOGY • BIOLOGY • PHYSICS
www.redjournal.org

BIOLOGY CONTRIBUTION

Ionizing Radiation Triggers the Antitumor Immunity by Inducing Gasdermin E-Mediated Pyroptosis in Tumor Cells

Wei Cao, MPhil,[*,†] Guodong Chen, PhD,[*,‡] Lijun Wu, PhD,[§] K.N. Yu, PhD,[‖,#] Mingyu Sun, BA,[*,¶] Miaomiao Yang, MPhil,[*] Yanyi Jiang, PhD,[*] Yuan Jiang, PhD,[*] Yuan Xu, MPhil,[*,†] Shengjie Peng, MPhil,[*,†] and Wei Han, PhD[*,‡,**]

[*]*Anhui Province Key Laboratory of Medical Physics and Technology, Institute of Health and Medical Technology, Hefei Institutes of Physical Science, Chinese Academy of Sciences, Hefei, P. R. China;* [†]*University of Science and Technology of China, Hefei, P. R. China;* [‡]*Hefei Cancer Hospital, Chinese Academy of Sciences, Hefei, P. R. China;* [§]*Institute of Physical Science and Information Technology, Anhui University;* [‖]*Department of Physics, City University of Hong Kong, Tat Chee Avenue, Kowloon Tong, Hong Kong, P.R. China;* [¶]*School of Basic Medical Science, Anhui Medical University, Hefei, Anhui, P. R. China;* [#]*State Key Laboratory in Marine Pollution, City University of Hong Kong, Tat Chee Avenue, Kowloon Tong, Hong Kong, P.R. China; and* [**]*Collaborative Innovation Center of Radiation Medicine of Jiangsu Higher Education Institutions and School for Radiological and Interdisciplinary Sciences (RAD-X), Soochow University, Suzhou, P. R. China*

Received Mar 6, 2022; Accepted for publication Jul 27, 2022

Purpose: To understand pyroptosis induced by ionizing radiation and its implications for radiation therapy, we explored the involved factors, possible mechanisms of radiation-induced pyroptosis and consequent antitumor immunity.

Methods and Materials: The occurrence of pyroptosis was assessed by cell morphology, lactate dehydrogenase release, Annexin V/PI staining and the cleavage of Gasdermin E (GSDME). Cell radiosensitivity was tested with MTT and colony survival assays. Xenograft tumor volume, Ki-67, $CD8^+$ lymphocytes, and ELISA were used to evaluate the effect of GSDME on tumor suppression after irradiation.

Results: Irradiation induced pyroptosis in GSDME high-expressing tumor cell lines covering lung, liver, breast, and glioma cancers. Cleavage of GSDME occurred in a dose- and time-dependent manner after irradiation, and pyroptosis could be induced by various kinds of irradiation. The combination of chemotherapy drugs for DNA damage (cisplatin or etoposide) or demethylation (decitabine or azacytidine) and irradiation significantly enhanced the occurrence of pyroptosis. Moreover, we revealed that the Caspase 9/Caspase 3/GSDME pathway was involved in irradiation-induced pyroptosis. Notably, enhanced tumor suppression was observed in Balb/c mice bearing GSDME-overexpressing 4T1 tumors compared with those bearing vector tumors for the promotion of antitumor immunity, which was manifested as distinctly elevated levels of cytotoxic T lymphocytes and release of the related cytokines rather than the direct effect of pyroptosis on tumor cell radiosensitivity.

Conclusions: As an immunogenic cell death caused by radiation, pyroptosis promotes antitumor immunity after irradiation. Our findings may provide new insights to improve the efficacy of tumor radiation therapy.

Corresponding author: Wei Han; E-mail: hanw@hfcas.ac.cn

Funding Statement: This study was financially supported by Natural Science Foundation of China (Nos. U20A20372 and 81974484).

Wei Cao and Guodong Chen made equal contributions to this study.

Disclosures: none.

Data Sharing Statement: Research data are stored in an institutional repository and will be shared upon request to the corresponding author.

Acknowledgments—We are grateful to Dr Feng Shao (National Institute of Biological Sciences, Beijing, China) for kindly providing the human GSDME plasmid.

Supplementary material associated with this article can be found, in the online version, at doi:10.1016/j.ijrobp.2022.07.1841.

Int J Radiation Oncol Biol Phys, Vol. 115, No. 2, pp. 440–452, 2023
0360-3016/$ - see front matter
https://doi.org/10.1016/j.ijrobp.2022.07.1841

Introduction

Radiation therapy (RT) is a major treatment for many cancers, including lung, esophageal, and head and neck. The effect of radiation therapy is mainly attributed to the inhibition of tumor cell growth and induction of cell death by ionizing radiation (IR) by promoting the production of reactive oxygen species (ROS) and causing DNA damage in the tumor cells. In recent decades, more types of programmed cell death, including autophagy, pyroptosis, and ferroptosis, have been reported. Beyond apoptosis, the roles of cell death in tumors are still under exploration.[1] Although different types of cell death are highly diverse in their phenotypes and modulating signal pathways, possible cross-links exist between these pathways to switch one type of cell death to an alternative one.[2] The differences between different death modes provide a new strategy for improving efficacy in cancer therapy. Furthermore, the antitumor immunity triggered by some cell death types, such as necroptosis, provides more insights into clinical cancer therapy, including the use of RT to induce whole-body effects on the inhibition of tumor growth.[3]

Pyroptosis, a kind of programmed cell death, is characterized by the formation of plasma membrane pores and the release of intracellular contents.[4] As the executors of pyroptosis, gasdermin family proteins, including GSDMA, GSDMB, GSDMC, GSDMD, GSDME, and Pejvakin, can form membrane pores and destroy the integrity of the cell membrane.[5] Among them, GSDMD, mainly expressed in immune cells, is cleaved by Caspase 1/Caspase 11 and mediates many inflammatory processes, such as infectious, autoimmune diseases, and tumors.[6] In recent years, GSDME has been reported to play an important role in pyroptosis induced by various stimuli, such as chemotherapeutic drugs, cold atmospheric plasma, photodynamic therapy, and CAR T-cells.[7-10] Caspase 3 has been shown to cleave GSDME and trigger pyroptosis in tumors with high GSDME expression but apoptosis in tumors with low GSDME expression.[11,12] In addition to Caspase 3, granzyme B (GzmB) is also able to cleave GSDME in target tumor cells.[13]

The immune system plays a critical role in the recognition and elimination of transformed malignant cells.[14] The antitumor immune response induced by immunotherapy, chemotherapy, and RT are beneficial in that they eliminate cancer cells and prevent metastasis and recurrence, thereby improving the prognosis of patients. Some types of radiation-induced cell death, sometimes also considered "in situ vaccination," contribute to the antitumor immune response after IR.[15] A large number of antigens released from dying irradiated tumor cells are presented by host antigen-presenting cells, such as CD169-positive macrophages, which can then trigger an antigen-specific immune response.[16] In addition, the damage-associated molecular patterns (such as HMGB1, heat shock protein, ATP, etc) released from dying cells after IR also promote the activation, migration and effect or function of antigen-specific killer T-cells by activating antigen-presenting cells (APCs), such as dendritic cells (DCs), mononuclear phagocytes and B cells.[17,18] However, not all modes of cancer cell death can induce an immune response. As a lytic and inflammatory type of programmed cell death, pyroptosis has been reported to elicit robust antitumor activity. Even less than 15% of tumor cells undergoing pyroptosis were confirmed to be sufficient to eliminate all 4T1 tumors in a mouse model.[19] Accumulating evidence demonstrates that pyroptosis induced by chemotherapeutic drugs and some small molecule drugs can act as a trigger for the antitumor immune response. However, whether RT induces pyroptosis in tumor cells remains unclear, and little is known about the role of pyroptosis in RT-induced antitumor immunity.

In this study, GSDME-mediated pyroptosis induced by IR was investigated. IR-induced pyroptosis in a time- and dose-dependent manner by activating the Caspase 9/Caspase 3/GSDME pathway. Importantly, we found that IR-induced pyroptosis boosted tumor suppression by initiating antitumor immunity, as shown by the enhanced activation of DCs and infiltration of cytotoxic T lymphocytes (CTLs) but did not sensitize tumor cells to irradiation. In addition, the combination of IR and chemotherapy or demethylated agents was identified as an effective strategy to increase the intensity of pyroptosis. We hope our study will be helpful for understanding pyroptosis induced by IR and will provide new insights into clinical RT.

Methods and Materials

Cell culture

PC-9, SF126, U251, HepG2, SF268, Huh-7, HCCLM3, MHCC-97L, T47D, THP1, 4T1, U87MG, MCF-7, MDA-MB-231, and HEK-293T cells were obtained from the Cell Bank of Type Culture Collection of the Chinese Academy of Sciences (Shanghai, China). H1299, Calu-1, A172, BT549, H460, H226, MDA-MB-468, and Hep3B cell lines were purchased from the American Type Culture Collection (Manassas, VA).

H1299, Calu-1, Huh-7, BT549, T47D, THP1, and 4T1 cells were cultured with RPMI-1640 medium (Gibco, Carlsbad, CA). PC-9, H460, H226, A172, SF126, SF268, U251, U87MG, HepG2, Hep3B, MHCC-97L, HCCLM3, MCF-7, MDA-MB-231, and MDA-MB-468 cells were cultured with DMEM (Gibco, Carlsbad,CA). All culture media were supplemented with 10% FBS (Lonsera, Uruguay), 100 μg/mL streptomycin and 100 U/mL penicillin. All cells were verified to be free of mycoplasma and cultured at 37°C in 5% CO_2.

Antibodies

The primary antibodies used in the present study, including anti-GSDMA (49307), anti-PARP (9532), anti-Caspase 3 (14220), anti-cleaved Caspase 3 (9661), anti-cleaved Caspase 7 (9491T), anti-Caspase 9 (9502), anti-GSDMB (76439), and

anti-GSDMD (96458), were purchased from CST (Beverly, MA). The anti-GSDME-N antibody (ab215191) was obtained from Abcam (Cambridge, MA). Anti-Caspase 7 (271551-1-AP), anti-Caspase 8 (13423-1-AP), and anti-β-actin were obtained from Proteintech (Wuhan, China). Anti-GSDMC (AP10771c) was purchased from Abgent (Suzhou, China). The anti-rabbit (926-32211) and anti-mouse (926-68070) secondary antibodies were purchased from Li-COR (Lincoln, NE). The antibodies against FITC-CD8a (100804), PerCP/Cyanine5.5-CD45 (1003132), and PE-CD3 (100206) were obtained from Biolegend (San Diego, CA). The antibody against mouse CD16/CD32 (553141) and Fixable Viability Stain 660 were obtained from BD (San Diego, CA). The antibodies against FITC-CD83 (121505), PE-CD40 (157505), PerCP/Cyanine7-CD86 (105014), APC-CD80 (104714), PE-CD335 (NKp46) (1137604), and FITC-CD49b (103504) were obtained from Biolegend.

Reagents

LPS (HY-D1056), cisplatin (HY-17394), etoposide (HY-13629), 5-fluorouracil (HY-90006), doxorubicin (HY-15142), and decitabine (HY-A0004) were purchased from MCE (New Jersey, USA). DNase I (DN25) and collagenase D (Colld-ro) were purchased from Sigma (New York, NY). Mouse TNF-α (M0002), IFN-γ (M0007), and GzmB ELISA Kits (M0594) were purchased from Elabscience (Wuhan, China). Recombinant murine granulocyte macrophage colony stimulating factor (GM-CSF) (315-03) and interleukin 4 (IL-4) (214-14) were purchased from Peprotech (East Windsor, NJ).

Irradiation

The cells cultured in dishes were irradiated with an X-ray irradiator (XHA600D, SHINVA, Zibo, China) at a dose rate of 1.88 Gy/min or a γ-ray irradiator (BIOBEAM GM2000, GSM, Germany) at a dose rate of 2 Gy/min. For α-particle irradiation (3 MeV, 0.067 Gy/min), the cells were cultured in dishes with a Mylar film (3.5 μm) bottom to facilitate penetration of α particles.

Western blotting

The cells were collected by centrifugation and lysed in RIPA buffer with PMSF (1 mM). The protein concentration was determined with a BCA Protein Assay Reagent Kit (Beyotime Biotechnology, Shanghai, China). The cell protein extracts were subjected to SDS-PAGE, transferred onto polyvinyl difluoride membranes, blocked with 5% nonfat dry milk, and subsequently incubated with primary antibodies at 4°C overnight. The membranes were incubated with secondary antibodies for 1 hour, and signals were detected with an Odyssey CLx Infrared Imaging System (Li-COR, Lincoln, NE).

Lactate dehydrogenase release assay

The lactate dehydrogenase (LDH) released was assayed with an LDH Cytotoxicity Assay Kit (C0017, Beyotime, Shanghai, China). In brief, the cells were irradiated and cultured for 48 hours, and the culture medium was then replaced with fresh culture medium with 1% FBS. At 72 hours after IR, the supernatant of the cell culture was collected for the detection of LDH activity according to the manufacturer's protocol.

Cell viability assay

Cell viability was assessed with a Cell Counting Kit-8 assay according to the manufacturer's recommendation.

ELISA

Tumors excised from Balb/c mice were pulverized and treated with PBS buffer for 10 min at 4°C. The mixture was centrifuged at 5000*g* at 4°C for 10 minutes, and the supernatants were collected for ELISA detection according to the manufacturer's instructions.

Small interfering RNA transfection

The siRNAs for Caspase 9 and Caspase 7 and the control siRNA were synthesized by GenePharma (Shanghai, China). The siRNA sequences of Caspase 9 were as follows: siRNA#1, CCAGGCAGCTGATCATAGA; siRNA#2, CGACCTGACTGCCAAGAAA. The siRNA sequences of Caspase 7 were as follows: siRNA#1, CCGUCCCUCUUCAGUAAGA; siRNA#2, UUUGCUGAAUCCUCAACCC. The cells were transfected with double-stranded siRNAs by using the Lipofectamine2000 transfection reagent (11668019, Thermo, CA) according to the manufacturer's protocol.

CRISPR/Cas9-mediated GSDME or Caspase 3 gene knockout

The GSDME or Caspase 3 knockout cell lines were established by using the CRISPR/Cas9 system. The target single guided RNA (sgRNA) sequence of GSDME was 5'-ATTCATAGACATGCCAGAT-3', and the sequence of Caspase 3 was 5'-AATGGCACAAACATTTGAAA-3'. These sgRNAs were cloned into the lenti-CRISPR V2 vector and then used to package lentivirus with pSPAX2 and pMD2G. Subsequently, PC-9 cells were infected with lentivirus and then cultured in DMEM complete medium containing 1 μg/mL puromycin for 14 days. Single surviving cells were plated into 96-well plates. After 2 weeks, the clones expanded from a single cell were detected for GSDME or Caspase 3 expression with western blotting. The clones without GSDME or Caspase 3 protein expression, named PC-9 KO GSDME or PC-9 KO Caspase 3, respectively, were selected for further experiments.

Establishing stable GSDME-overexpressing cells

The human GSDME plasmid (a kind gift from Dr F. Shao, National Institute of Biological Sciences, Beijing, China) was constructed by inserting cDNAs of human GSDME (hGSDME) into a pWPI-2 × Flag-HA lentiviral vector. A mouse GSDME plasmid was constructed by inserting mouse GSDME (mGSDME) cDNAs (NM_018769.4) into a PCDH-CMV-MCS-EF1-CopGFP-T2A-Puro lentiviral vector plasmid (Miaolingbio, Wuhan, China). To generate lentiviruses, the GSDME plasmid or the corresponding empty vector plasmid was transfected into HEK293T cells with pSPAX2 and pMD2G at a ratio of 5:3:2. Lentivirus-containing supernatant collected at 48 hours after transfection was used to infect cells for 48 hours. The infected cells were then cultured in DMEM containing 2 μg/mL puromycin for 14 days to obtain hGSDME-overexpressing H1299 cells (H1299 GSDME). A stable 4T1 cell line overexpressing mGSDME was also established with the same method.

Flow cytometry for cell death detection

The cells were collected and washed with PBS at 72 hours after irradiation. Subsequently, the cells were resuspended in binding buffer and stained with Annexin V-FITC/propidium iodide (PI) (BD Sciences, San Diego, CA) for flow cytometry according to the manufacturer's instructions. Data were processed with FlowJo software.

Detection of tumor-infiltrated immune cells

Tumors excised from Balb/c mice were cut and treated with DMEM containing 2 mg/mL collagenase D, 100 μg/mL DNase I, and 1% FBS at 37°C for 30 minutes with agitation. Tumor fragments were collected and filtered with 70 μm strainers, and the filtered cells were then treated with red blood cell lysis buffer (Beyotime Biotechnology, Shanghai, China) and washed twice with FACS buffer (PBS with 2% FBS). Single-cell suspensions prepared as previously described were incubated with antimouse CD16/CD32 for 30 minutes at 4°C and then incubated for 30 minutes at 4°C with antibodies against CD45, CD8-a, and CD3. Dead cells were excluded using Fixable Viability Stain 660 supplemented with antibodies. Cells prepared as previously described were washed twice and resuspended in FACS buffer (PBS with 2% FBS) and then analyzed by flow cytometry. Data were processed with FlowJo software.

RNA extraction and quantitative real-time PCR

Total RNA was isolated from cells with a RNeasy Mini kit (Qiagen, Germany), and cDNAs were synthesized from 2 μg of total RNA with a NovoScript 1st Strand cDNA Synthesis kit (Novoprotein, Shanghai, China).

Real-time PCR was performed with One Step SYBR PrimeScriptTM RT-PCR Kits (Takara Bio, Dalian, China) on a Roche 480 Light Cycler (Roche, Basel, Switzerland). The primers for PCR amplification are shown as follows: 5'-ACATGCAGGTCGAGGAGAAGT-3', 5'-TCAATGACACCGTAGGCAATG-3' (GSDME); 5'-TGCACACCAGGACCCTATCC-3', 5'-GAGGCTGACAGGCTGCAGATGT-3' (H2-D1), 5'-ACGTGGCGGCGATTATCAC-3', 5'-`AGGTAGGCCCTGTAATACTCTG-3' (H2-Q10), and 5'-CTGGGACGACATGGAGAAAA-3', 5'-AAGGAAGGCTGGAAGAGTGC-3' (Actin). The *actin* gene was used as a control, and the data are presented as fold changes in gene expression in the tested samples compared with the control with the $2^{-\Delta\Delta Ct}$ method.

Tumor growth and treatments

Six-week-old female Balb/c-nude and Balb/c mice (GemPharmatech, Nanjing, China) were used to graft 4T1 vector or 4T1 mGSDME cells (5×10^6) by subcutaneous injection into the right flank. When tumors reached a size of ~200 mm^3, they were irradiated with 3 × 8 Gy X-ray. Tumor growth was monitored by measuring the volume of tumors every 2 days.

The volume of the tumor was calculated as $(L \times S^2)/2$, where L was the longest length and S was the shortest length. The mice were killed at day 36 after the cell injection, and all tumors were excised.

Culture of bone marrow-derived dendritic cells

Bone marrow-derived dendritic cells (BMDCs) were obtained as previously described.[20] In brief, the femurs and tibiae of Balb/c mice were isolated from surrounding muscle tissues and washed twice in PBS. Both joints were cut to expose the marrow cavity, and the cells in the cavity were blown out with RPMI 1640 medium with a 1 mL syringe. A total of 1×10^7 cells were cultured in RPMI 1640 supplemented with GM-CSF (10 ng/mL), IL-4 (10 ng/mL), FBS (10%), streptomycin (100 μg/mL), and penicillin (100 U/mL). After 24 hours of incubation, nonadherent cells were discarded, and the medium was replaced with fresh medium. On day 6, flow cytometry analysis was conducted to test the cell purity of the separated BMDCs.

Co-culture system of tumor cells and BMDCs

BMDCs (3×10^5 cells per well) and tumor cells (5×10^5 cells per insert) were seeded into 6-well plates and Transwell inserts, respectively. Before IR treatment, the medium in the wells and inserts was replaced with fresh complete medium. Immediately after IR (10 Gy), the Transwell inserts were placed into 6-well plates for co-culture. The DCs were then detected with flow cytometry after 72 hours.

Immunohistochemistry

The tumor sections (5 μm) were deparaffinized in xylene, rehydrated through gradient ethanol and then stained with Ki-67 (Keygen Biotech, Nanjing, China), CD8 (MA1-7632, Novusbio Biologicals, Littleton, CO), CD4 (MHCD0400, Novusbio Biologicals, Littleton, CO), and CD68 (28058-1-AP, Proteintech, Wuhan, China) detection immunohistochemistry kits (KIT-5010, MXB Biotechnologies, Fuzhou, China) according to the manufacturers' instructions.

Statistical analysis

All experiments were performed at least 3 times. All analyses were performed with GraphPad Prism statistical software. For all experiments, comparisons between 2 groups were based on a paired sample *t* test, and one-way analysis of variance was used to test the difference between 3 or more groups. Comparisons between 2 groups were based on *t* tests. Data are shown as the means ± standard deviation.

Results

IR induces pyroptosis in various cancer cell lines with high GSDME expression

Gasdermin family proteins, including GSDMA, GSDMB, GSDMC, GSDMD, and GSDME, are considered executors of pyroptosis.[5] In this study, the constitutive expression of GSDMA, GSDMB, GSDMC, GSDMD, and GSDME was first screened in 20 cancer cell lines in total covering liver (MHCC-97L, Huh-7, Hep3B, HCCLM3, and HepG2), lung (H1299, PC-9, Calu-1, H460, and H226), glioma (A172, U87MG, U251, SF268 and SF126), and breast (MDA-MB-468, BT549, MDA-MB-231, T47D and MCF-7) cancers. As shown in Figure E1A-D, GSDMA, GSDMB, and GSDMC proteins could not be observed in any of the examined cell lines, and GSDMD proteins could only be observed in some of these cell lines. However, GSDME proteins were detected in most of these tested cell lines (Fig. 1A). These results indicate that GSDMD or GSDME may be involved if pyroptosis can be induced by X-ray irradiation. Indeed, we found obvious cleavages of GSDME after IR in cells with high GSDME expression (Fig. 1A). Nonetheless, the cleavage of GSDMD was not observed after IR in MDA-MB-231 and HCCLM3 cells (Fig. E1E), although both GSDMD and GSMDE were highly expressed in these 2 cell lines. To further clarify the role of GSDME in IR-induced pyroptosis, 4 pairs of cell lines (PC-9/H1299, HepG2/MHCC-97 L, SF126/U251, and MCF-7/MDA-MB-468) with relatively high or low GSDME expression were selected for further detection. The typical morphologic characteristics of pyroptosis, including cell swelling and the formation of large bubbles from the plasma membrane, were observed in cancer cells with high GSDME expression but not in those with low GSDME expression (Figs. 1B). In pyroptotic cells losing membrane integrity by gasdermin-mediated membrane pore formation, increased Annexin V/PI double-positive cells and LDH release have been observed.[5] Coincidently, in our study, the proportion of Annexin V/PI double-positive cells and the release of LDH in cells with high GSDME expression were also significantly higher than those in cells with low GSDME expression (Fig. 1C-E). These results suggest that IR induces pyroptosis in cancer cells with high GSDME expression.

IR induces pyroptosis in a dose- and time-dependent manner

The dose- and time-dependent effects of IR-induced pyroptosis were then explored. The cleavage of GSDME showed a dose-dependent increase in cells with high GSDME expression (PC-9, HepG2, and SF126) after exposure to a series of IR doses (Fig. 2A, Fig. E2B). Considering the important clinical use of different dose fractions of IR, we next evaluated pyroptosis induction after exposure to the same total IR dose but different dose fractions (1 × 10 Gy/d vs. 5 × 2 Gy/d). As shown in Figure 2B, a single fraction of 10 Gy promoted more GSDME cleavages compared with multiple fractions, indicating that a large IR dose fraction is more effective than conventional IR dose fractions in pyroptosis induction. In addition to X-ray, γ-ray, and α particles also exhibited a similar effect on GSDME cleavage and pyroptosis induction in tumor cells (Fig. 2C, D). With a typical dose (10 Gy) of IR, the level of GSDME-N continued to increase in PC-9, HepG2, and SF126 cells 96 hours after IR (Fig. 2E, Fig. E2C), indicating a time-dependent pyroptosis induction.

GSDME mediates IR-induced pyroptosis

To further confirm the critical role of GSDME in IR-induced pyroptosis, we generated GSDME knockout PC-9 cells (PC-9 KO GSDME) and GSDME-overexpressing H1299 cells (H1299 GSDME). As shown in Figure 3, PC-9 KO GSDME cells displayed a distinct reduction in cell swelling (Fig. 3A), ratio of Annexin V/PI double-positive cells (Fig. 3B, Fig. E2E), LDH release (Fig. 3C) and GSDME-N levels (Fig. 3D) after IR compared with the negative control (NC) cells. In contrast, H1299 GSDME cells displayed more cell swelling (Fig. 3A), elevated GSDME-N protein levels (Fig. 3D), more released LDH (Fig. 3C), and more Annexin V/PI double-positive cells (Fig. 3B, Fig. E2D) compared with H1299 vector cells after IR. These results indicate that GSDME is necessary for IR-induced pyroptosis. To further explore the role of GSDME in IR-induced pyroptosis, we overexpressed mGSDME in mouse breast cancer 4T1 cells (4T1 mGSDME) (Fig. 3E). The results of *in vitro* experiments (Fig. 3E, Fig. E2F) also showed that overexpressing mGSDME in 4T1 cells significantly enhanced IR-induced pyroptosis.

Given that the expression of GSDME is usually suppressed in various cancers due to methylation of its

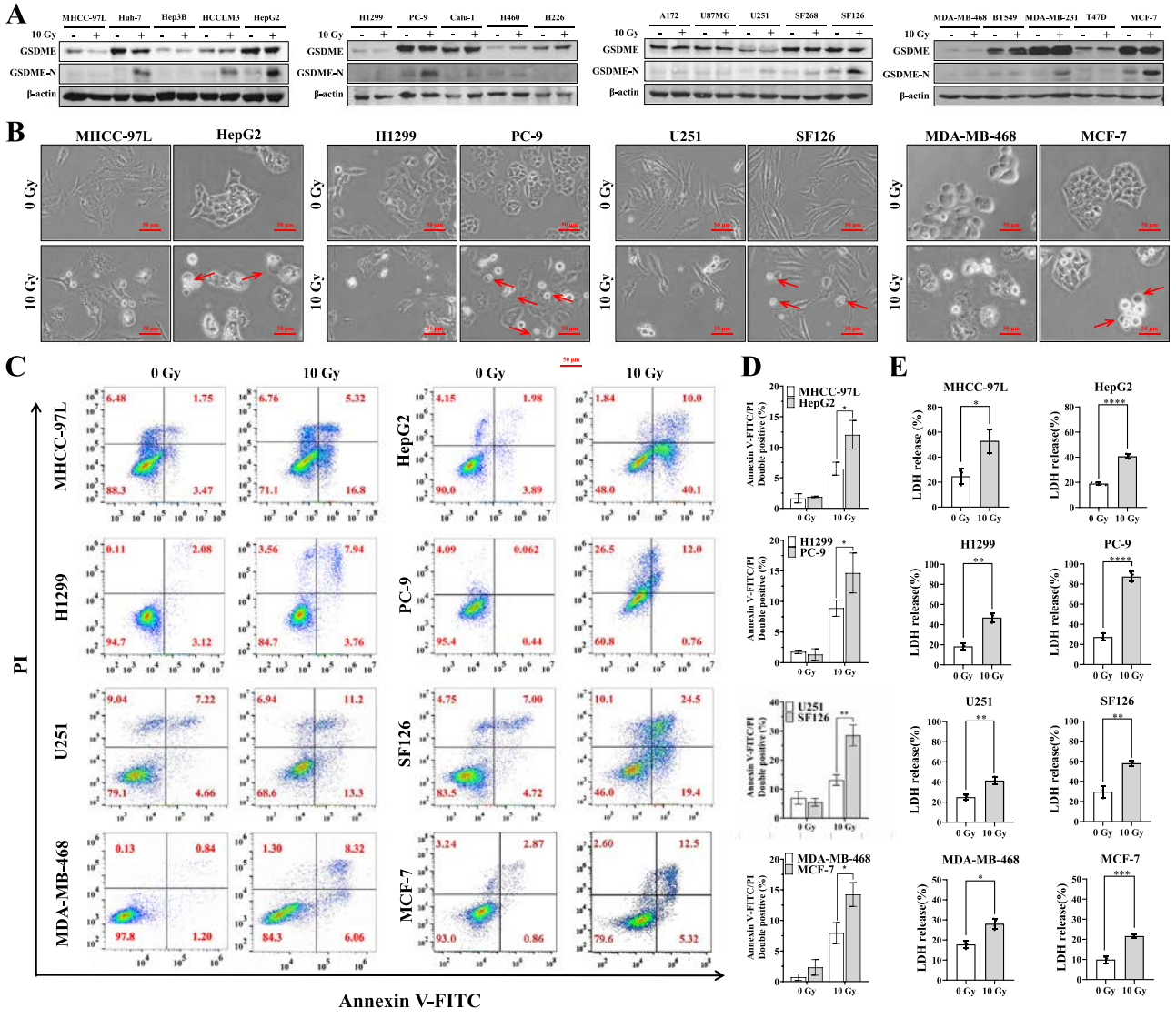

Fig. 1. Pyroptosis induced by IR (X-ray) in tested cancer cell lines. (A) Expressions of GSDME and GSDME-N at 72 hours after IR (10 Gy). (B) Representative images of 4 pairs of cell lines with high/low GSDME expression captured at 72 hours after IR (10 Gy). Red arrows indicate the large bubbles emerging from the plasma membrane. (C) Flow cytometry analysis of cell death stained with Annexin V/PI. (D) Quantified results of (C). (E) Lactate dehydrogenase released from irradiated cells. $^{*}P < .05$, $^{**}P < .01$, $^{***}P < .001$.

promoter DNA,[21] we speculated that DNA demethylation agents might promote the expression of GSDME in cancer cell lines with low GSDME expression. As expected, we found that GSDME expression was enhanced after treatment with decitabine (5 μM) or azacytidine (10 μM) in MDA-MB-468 cells (Fig. 3F). Moreover, increased GSDME cleavage was also observed after IR in MDA-MB-468 cells pretreated with azacytidine or decitabine. Considering the common combination of radio- and chemotherapy in clinical use, we further evaluated the effect of some other drugs often used in cancer chemotherapy on IR-induced pyroptosis. As shown in Figure 3G, the combination of IR with cisplatin or etoposide rather than 5-FU or doxorubicin boosted GSDME cleavage in PC-9 cells. Collectively, these results reveal that IR combined with DNA demethylation agents or some other chemotherapy agents could enhance IR-induced pyroptosis. Interestingly, the mRNA expression of GSDME was upregulated in MCF-7 and MDA-MB-231 cells after IR, indicating that IR can enhance GSDME expression in some cancer cell lines (Fig. 3H).

GSDME mediates IR-induced pyroptosis through the Caspase 9/Caspase 3 pathway

Caspase 3 activation has been reported to trigger both apoptosis and pyroptosis by cleaving PARP and GSDME, respectively.[7] Indeed, we found not only activated Caspase 3 and cleaved GSDME but also cleaved PARP in irradiated PC-9 cells (Fig. 4A), implying that IR induced both

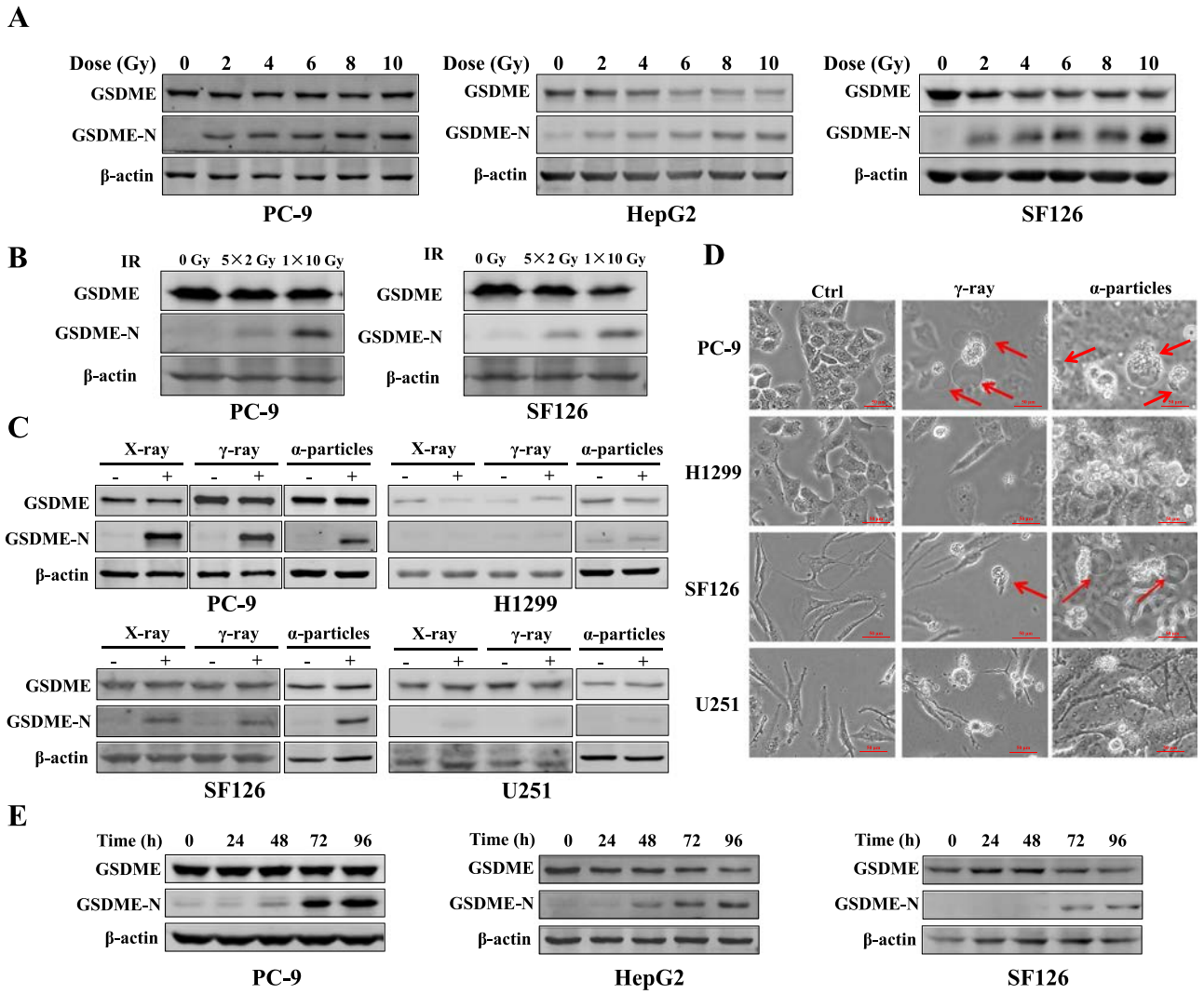

Fig. 2. IR induces pyroptosis in a dose- and time-dependent manner. (A) Expressions of GSDME and GSDME-N in PC-9, HepG2, and SF126 cells at 72 hours after a range dose of IR (X-ray, 0-10 Gy). (B) Expressions of GSDME and GSDME-N in PC-9 and SF126 cells 72 hours after a single or fractioned IR (X-ray). (C) Expressions of GSDME and GSDME-N in PC-9, HepG2, and SF126 cells 72 hours after X, γ-ray or α particles irradiation. (D) Representative images of PC-9, H1299, SF126, and U251 cells irradiated with γ-ray or α particles. Scale bar: 50 μm. (E) Expressions of GSDME and GSDME-N proteins detected at indicated time points after IR (x-ray, 10 Gy) in PC-9, HepG2, and SF126 cells.

apoptosis and pyroptosis. In addition, to investigate the upstream targets of Caspase 3, activation of Caspase 8 (receptor-mediated death pathways) and Caspase 9 (mitochondrial death pathway) were also detected. The results (Fig. 4A) showed a distinct increase in cleaved Caspase 9 but not Caspase 8 after IR, suggesting that the mitochondrial death pathway might trigger IR-induced apoptosis/pyroptosis. This conclusion was also supported by the increased level of Bax protein after IR (Fig. 4A).

To further confirm the critical role of Caspase 3 in IR-induced apoptosis/pyroptosis, we knocked out Caspase 3 in PC-9 cells by using the CRISPR/Cas9 system. Notably, Caspase 3 KO completely suppressed the cleavage of GSDME but only partially reduced the cleavage of PARP (Fig. 4B), providing strong evidence that activation of Caspase 3 is indispensable for IR-induced pyroptosis but not apoptosis. Moreover, the distinct reduction in pyroptosis characteristics, including cell swelling (Fig. E2G), the proportion of Annexin V/PI double-positive cells and LDH release (Fig. 4C-E) after IR in the absence of Caspase 3 also further proved the key role of Caspase 3 in IR-induced pyroptosis. In line with these results, we noticed that Caspase 7, known as the other Caspase except Caspase 3 responsible for PARP cleavage, was also activated after IR (Fig. 4B), possibly explaining the cleavage of PARP in the absence of Caspase 3. Subsequently, Caspase 7 specific siRNA was employed to interfere with the expression of Caspase 7 in Caspase 3 KO cells to determine the possible involvement of Caspase 7 in IR-induced apoptosis. As shown in Fig. 4F, a significant decrease in cleaved PARP was observed in Caspase 7 knockdown cells compared with the control, confirming the involvement of Caspase 7 in IR-induced apoptosis. We also

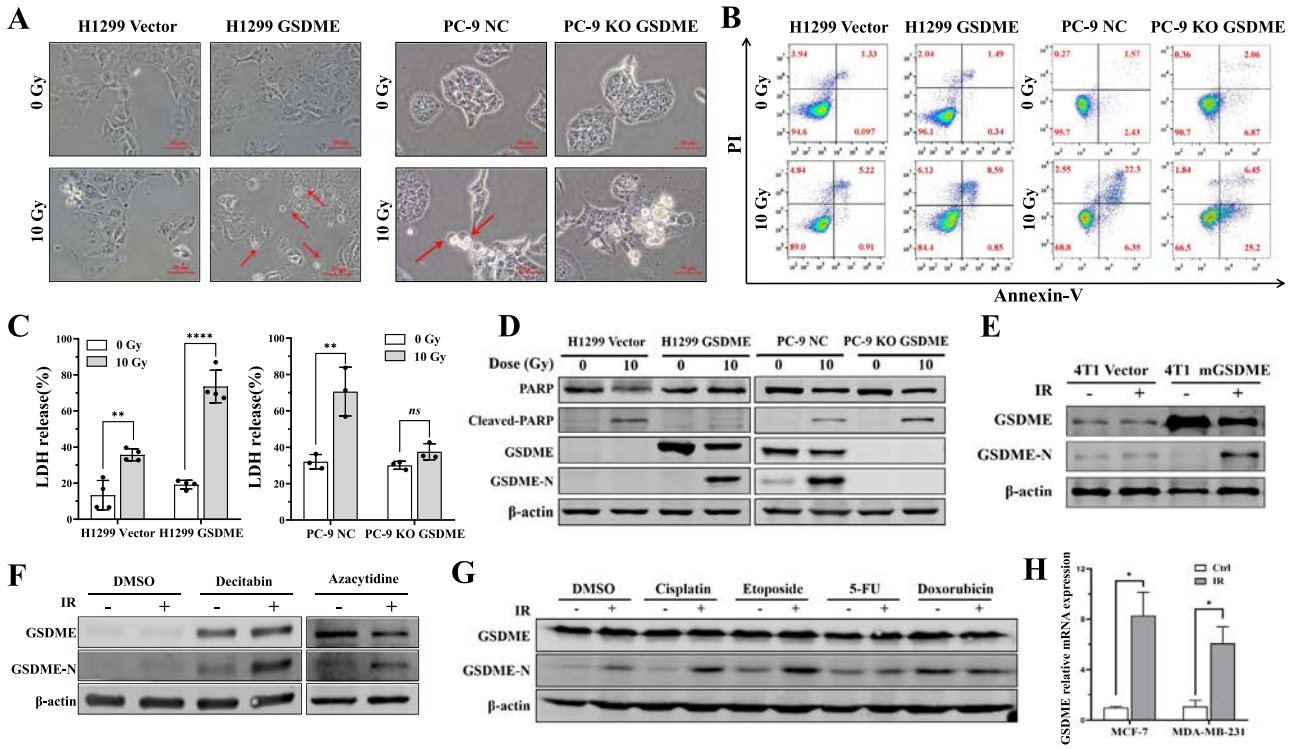

Fig. 3. GSDME mediates pyroptosis after IR (X-ray). (A) Representative images of H1299 vector/H1299 GSDME and PC-9 NC/PC-9 KO GSDME cells after IR (10 Gy). Scale bar: 50 μm. (B) Flow cytometry assay of cell death stained with Annexin V/PI. (C) Lactate dehydrogenase release and (D) expressions of indicated proteins after IR (10 Gy). Expressions of GSDME and GSDME-N in 4T1 vector and 4T1 mGSDME cells (E) and MDA-MB-468 cells (F), with decitabine or azacytidine pretreatment for 72 hours, detected at 72 hours after IR (10 Gy). (G) Expressions of GSDME and GSDME-N in PC-9 cells detected at 72 hours after treatment with the combination of different chemotherapy drugs and IR (10 Gy). (H) Transcription levels of GSDME detected at 72 hours after IR (10 Gy) in MCF-7 and MDA-MB-231 cells. *Abbreviation*: ns = not significant. $^{*}P < .05$, $^{**}P < .01$, $^{***}P < .001$.

further examined the effect of Caspase 9 on promoting IR-induced apoptosis and pyroptosis by knocking down Caspase 9. Caspase 9 knockdown cells displayed less cleavage of Caspase 3, Caspase 7, GSDME, and PARP, which suggests Caspase 9 played a key role in triggering IR-induced apoptosis and pyroptosis (Fig. 4G).

Overall, our results revealed that IR induced both apoptosis and pyroptosis in tumor cells with high GSDME expression when Caspase 9 triggered the Caspase 3/GSDME and Caspase 3/7/PARP pathways, respectively. Furthermore, we found that apoptosis mediated by Caspase 7 did not switch to pyroptosis, even in the presence of high GSDME expression.

GSDME-mediated pyroptosis boosts tumor suppression by triggering antitumor immunity rather than the direct cell killing effect of IR

To explore the role of GSDME-mediated pyroptosis in radiotherapy, we injected 4T1 mGSDME or 4T1 vector cells into Balb/c mice. After 3 × 8 Gy IR, stronger inhibition of tumor growth was determined by tumor volume and tumor weight (Fig. 5A-C); immunohistochemistry (IHC) of Ki-67 (Fig. 5F, G) was observed in mGSDME-overexpressing 4T1 tumors compared with 4T1 vector tumors. Meanwhile, distinct cleavage of GSDME was detected after IR in mGSDME-overexpressing 4T1 tumors (Fig. 5D, E). These results suggest that GSDME-mediated pyroptosis enhances tumor suppression after radiation.

Considering that enhanced pyroptosis might elevate the radiosensitivity of tumor cells, we tested the colony survival and cell viability of tumor cells after irradiation. Surprisingly, overexpression of GSDME/mGSDME in H1299 and 4T1 cells, respectively, did not reduce the cell viability or survival fraction after irradiation though distinct pyroptosis (Fig. 5H, I; Fig. E3A, B). The results of the *in vivo* experiment, performed in the subcutaneous tumor model of Balb/c nude mice, showed that mGSDME-overexpressing 4T1 tumors did not display a stronger inhibitory effect of IR (3 × 8 Gy) on tumor growth, as evaluated by tumor volume and IHC of Ki-67, than 4T1 vector tumors (Fig. 5J-N). A similar result was also shown in GSDME-overexpressing and vector H1299 xenografted models of Balb/c nude mice (Fig. E3C-I). These results suggest that GSDME-mediated pyroptosis did not change the radiosensitivity of tumor cells.

Considering the possibility of antitumor immunity activation in the mGSDME-overexpressing 4T1 subcutaneous

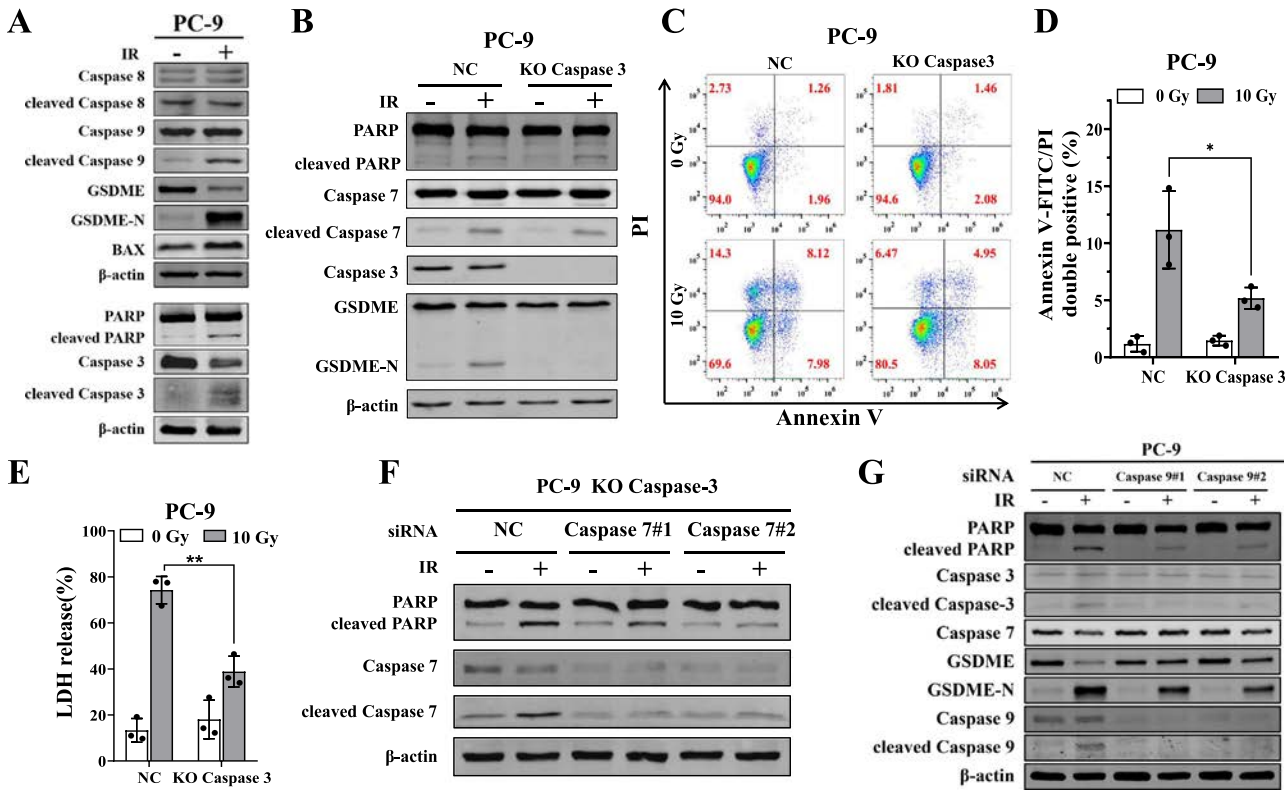

Fig. 4. GSDME mediates IR-induced pyroptosis through Caspase 9/Caspase 3 pathway. (A) Expressions of apoptotic and pyroptotic related proteins in PC-9 cells detected at 72 hours after IR (10 Gy X-ray). (B) Expressions of apoptotic and pyroptotic related proteins in PC-9 NC and PC-9 KO Caspase 3 cells detected at 72 hours after IR (10 Gy). (C) Flow cytometry assay of cell death stained with Annexin V/PI and the quantification (D), and lactate dehydrogenase release (E) from PC-9 NC and PC-9 KO Caspase 3 cells at 72 hours after IR (10 Gy). The expressions of indicated proteins in PC-9 KO Caspase 3 or PC-9 cells transfected with Caspase 7 siRNA (F) or Caspase 9 siRNA (G) detected at 72 hours after IR (10 Gy). $^{*}P < .05$, $^{**}P < .01$.

tumors after IR causing further suppression of tumor growth, we detected the infiltration of immune cells, including T lymphocytes, NK cells and macrophages, in the irradiated tumors (Balb/c mice) with flow cytometry and immunohistochemistry. The results in Figures 6A and 6B showed that more $CD8^+$ T lymphocytes but no more NK cells after IR were observed in mGSDME-overexpressing 4T1 tumors than 4T1 vector tumors. In addition, there were no significant differences in the infiltration of $CD4^+$ T-cells and macrophages between irradiated 4T1 mGSDME tumors and irradiated 4T1 vector tumors in Balb/c mice after IR (Fig. 6D, E). These results indicated that $CD8^+$ T-cells may play an important role in antitumor immunity, which was also confirmed by the results that Granzyme B, TNF-α and INF-γ (Fig. 6F), important antitumor molecules released by cytotoxic T-cells, were also significantly increased in irradiated 4T1 mGSDME tumors but not in irradiated 4T1 vector tumors.

Next, we assessed the expression of MHC class I molecules (H2-Q10 and H2-D1), which were reported to be involved in the immune response against tumors by interacting with $CD8^+$ T-cells,[22] in 4T1 vector cells and 4T1 mGSDME cells after IR. No significant difference in the expression of H2-Q10 and H2-D1 was observed between the irradiated 4T1 vector cells and irradiated 4T1 mGSDME cells (Fig. 6G), suggesting that overexpressing GSDME does not change the immunologic "visibility" of tumor cells.

Given that DCs play a critical role in antigen presentation, which is required for the activation of $CD8^+$ T-cells, the expression of DC surface antigens such as CD40, CD83, CD86, and CD80, markers of mature and activated DCs,[23,24] was detected after coculture with irradiated tumor cells (Fig. 6H). As expected, we found that the expression of all these markers was elevated after coculture with irradiated 4T1 mGSDME cells but not irradiated 4T1 vector cells (Fig. 6I), indicating that GSDME-mediated pyroptosis after IR enhances the antigen presentation of DCs.

Taken together, our results indicate that GSDME-mediated pyroptosis effectively promotes the infiltration of $CD8^+$ T lymphocytes by enhancing the antigen presentation of DCs but not NK cells, $CD4^+$ T lymphocytes or macrophages, thereby boosting antitumor immunity after irradiation.

Discussion

Radiation is conventionally considered to suppress activation of the immune system, while accumulating evidence indicates activated antitumor immunity after RT under

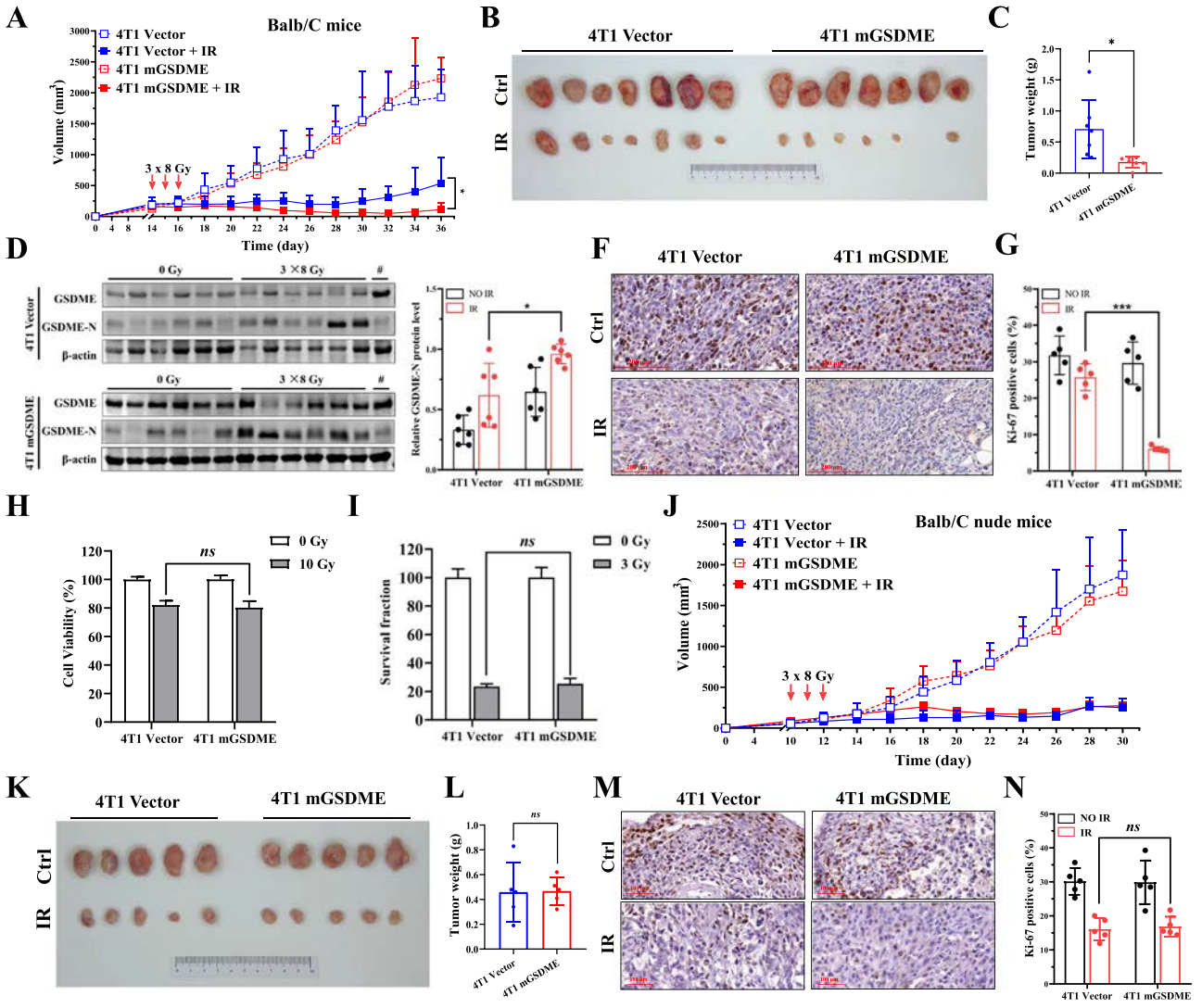

Fig. 5. GSDME-mediated pyroptosis boosts tumor suppression by triggering antitumor immunity. Growth curves (A), tumor images (B) and weights (C) in Balb/c mice bearing 4T1 vector/4T1 mGSDME with or without IR treatment. (D) Expressions of GSDME/GSDME-N and quantification (E) in 4T1 vector/4T1 mGSDME tumors cut from Balb/c mice. 4T1 mGSDME tumor protein described as the number was set as positive control. Representative immunohistochemistry images of Ki-67 (F) and quantification (G) of the positive cells in tumors cut from Balb/c mice. Cell viability (H) and clonogenic survival (I) of 4T1 vector and 4T1 mGSDME cells after IR. Growth curves (J), tumor images (K), and weights (L) in Balb/c nude mice bearing 4T1 vector /4T1 mGSDME with or without IR. Representative immunohistochemistry images of Ki-67 (M) and quantification (N) of the positive cells in tumors cut from Balb/c nude mice. *Abbreviation*: ns = not significant, $^{*}P < .05$, $^{**}P < .01$, $^{***}P < .001$.

some circumstances.[25] The genetic characteristics of tumors and the dose/dose fraction of IR, etc, are believed to play important roles in triggering antitumor immunity after RT.[26] As one member of the gasdermin family of proteins, GSDME-mediated pyroptosis has also been considered for its important role in immunoregulation. Zhang et al showed that even slight pyroptosis initiated by spontaneous apoptosis or immune-mediated killing in mouse-derived GSDME-overexpressing tumor cells, in the absence of any extrinsic stimuli, could boost antitumor immune responses to inhibit tumor growth.[13] Although this inhibition of tumor growth was not observed in our study (Fig. 5A, B), enhanced cleavage of GSDME and slightly increased $CD8^+$ T lymphocytes were observed in some nonirradiated GSDME-overexpressing Balb/c mouse tumors compared with vector tumors (Figs. 5E and 6A). We speculated that the extremely low level of spontaneous pyroptosis mediated by GSDME in some mouse tumors might not be enough to significantly inhibit tumor growth in our study. Indeed, after IR treatment of GSDME-overexpressing 4T1 tumors, significant pyroptosis in tumors and an enhanced antitumor immune response, including increased $CD8^+$ T lymphocyte infiltration and levels of TNF-α, IFN-γ and granzyme B in tumors, were found. Previous studies reported similar results in GSDME-positive tumors after cisplatin or BRAFi + MEKi treatment.[27,28] Furthermore, a difference in recruited

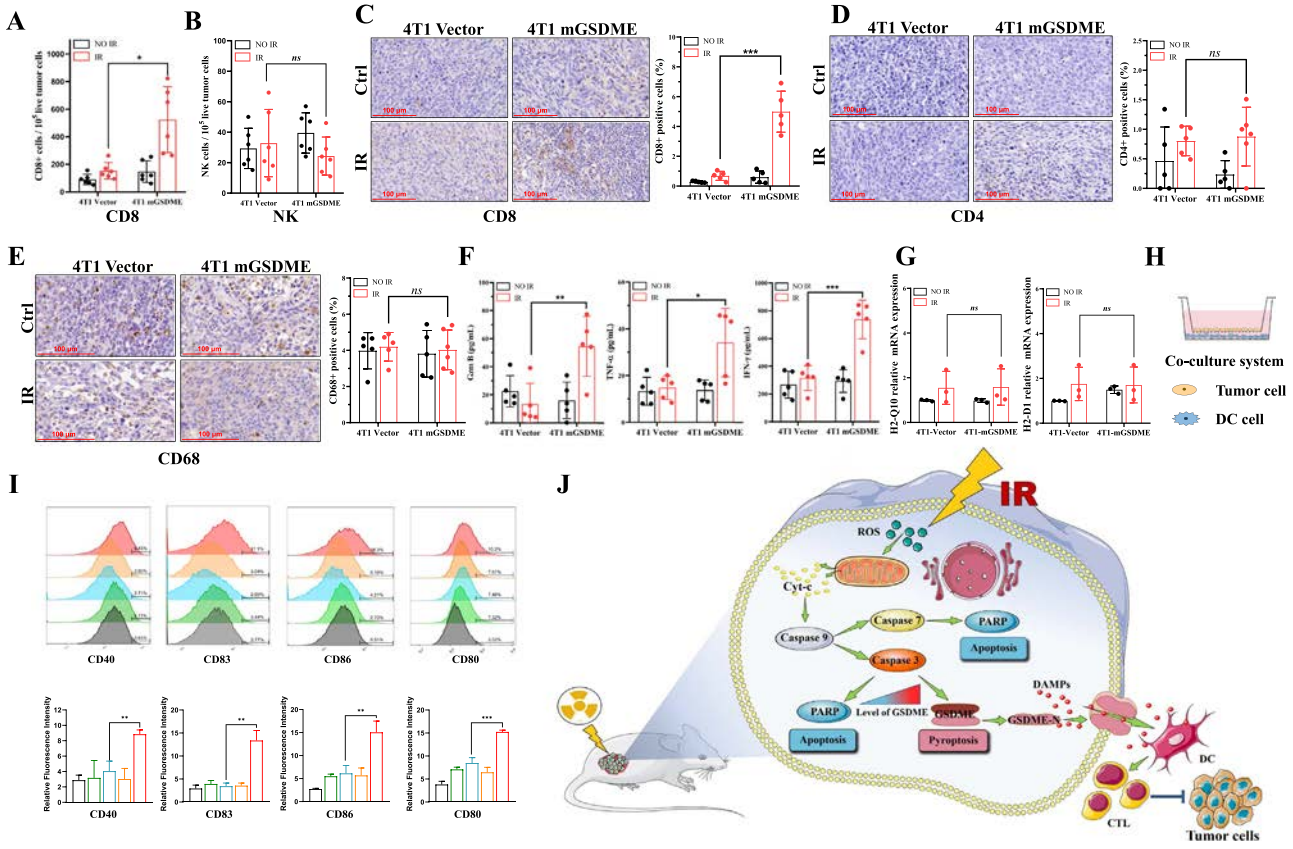

Fig. 6. GSDME-mediated pyroptosis activates the antitumor immunity. Numbers of $CD8^+$ T-cells (A) and NK cells (B) per 10^5 cells in tumors cut from Balb/c mice at day 8 after last IR. (C) Representative immunohistochemistry (IHC) images of $CD8^+$ T-cells and the quantification of the positive cells. Scale bar: 100 μm. (D) Representative IHC images of $CD4^+$ T-cells and quantification of the positive cells. Scale bar: 100 μm. (E) Representative IHC images of CD68 and quantification of the positive cells. Scale bar: 100 μm. (F) Levels of Gzm B, TNF-α and IFN-γ determined with ELISA in tumors cut from Balb/c mice. (G) Transcription levels of H2-Q10 and H2-D1 detected at 72 hours after IR (10 Gy) in 4T1 vector and 4T1 mGSDME cells. (H) The coculture system of DCs and tumor cells. (I) Representative images of flow cytometry assay for CD40, CD83, CD86, and CD80 and the quantification of activated DCs based on the relative fluorescence intensity. (J) Schematic overview of mechanism underlying the trigger of antitumor immunity by IR through inducing GSDME-mediated pyroptosis in tumor cells. *Abbreviation:* ns = not significant. $^*P < .05$, $^{**}P < .01$, $^{***}P < .001$.

immune effector cells triggered by pyroptosis after different stimuli was noticed. Erkes DA reported that BRAFi + MEKi treatment-induced pyroptosis accelerated the proliferation of $CD8^+$ and $CD4^+$ T-cells.[27,28] Spontaneous pyroptosis was found to enhance the number and function of tumor-infiltrated lymphocytes (NK cells and $CD8^+$ T lymphocytes) and macrophage-mediated phagocytosis.[13] Pyroptosis induced by IR (4 × 2 Gy) was reported to promote the infiltration of NK cells in colon tumors in mice,[29] whereas pyroptosis initiated by IR (3 × 8 Gy) recruited $CD8^+$ T-cells but not NK cells or $CD4^+$ T-cells in breast tumors in our study. Given the different and complex responses of antitumor immunity to the stimuli to the tumor, more involved factors beyond pyroptosis should be considered in the activation of antitumor immunity.

Considering the downregulation of GSDME by hypermethylation of its promoter region in many cancers,[30] the low expression level of GSDME is regarded as a primary obstacle to inducing pyroptosis. Azacytidine and decitabine, DNA hypomethylating agents used clinically, have been reported to elevate the expression of GSDME.[31] Similarly, azacytidine or decitabine promoted GSDME expression, and either of them combined with IR also induced more pyroptosis in our study (Fig. 3G). Existing evidence also showed that decitabine enhanced T-cell-mediated cytotoxicity and the release of IFN-γ against target tumor cells after IR.[32] Moreover, our data also indicate that some chemotherapeutic drugs, such as cisplatin and etoposide, also enhance the cleavage of GSDME induced by IR (Fig. 3G). This was consistent with some previous studies showing that combined chemoradiotherapy (carboplatin or paclitaxel plus IR) increased immunogenic cell death and enhanced proimmunogenic signaling from dying tumor cells.[33] However, some clinical studies also indicated that chemo- (platinum or 5-FU) radiation therapy significantly upregulated PD-L1 expression in tumors along with the increase in $CD8^+$ tumor-infiltrating lymphocytes[34,35] or even stimulated the recurrence or metastasis of tumors by suppressing

antitumor immunity.[36,37] The combined treatment of stereotactic body radiation therapy (SBRT) plus pembrolizumab, an anti-PD-1 antibody, and trametinib (in phase 2 trials) has been proven to extend the median overall survival of patients with locally recurrent pancreatic cancer,[38] suggesting that the combination of chemoradiotherapy and immune checkpoint inhibitors may be a promising strategy for cancer treatment in the future. In addition, several clinical reports have investigated the relationship between different $CD8^+$ T-cell immunophenotypes, such as T_{TR}, T_{CM}, T_{EM}, and T_N, and clinical outcomes. The T_{TR} immunophenotype was discovered to play an important antitumor role and may be a target for anti-PD-1 immunotherapy.[39,40] Accordingly, more factors beyond pyroptosis of tumor cells, such as antigen release and $CD8^+$ T-cell immunophenotype, should be considered when evaluating the effect of chemoradiotherapy on antitumor immunity.

Increasing evidence has revealed the important role of the segmentation mode of IR dose, an important clinical parameter associated with prognosis, in driving antitumor immunity by inducing many types of tumor cell death beyond apoptosis and necrosis; high-dose fractionated IR showed stronger effects than conventional fractionated IR.[41,42] This is also supported by our results that a single dose of 10 Gy resulted in stronger pyroptosis than conventional fractionated IR (5 × 2 Gy) (Fig. 2B). Although the fractionated radiation treatment regimen of 3 × 8 Gy has been proven to effectively induce antitumor immunity in some previous studies,[42,43] the infiltration of $CD8^+$ T lymphocytes was not significantly increased in the irradiated 4T1 vector (3 × 8 Gy) group compared with the nonirradiated 4T1 vector group in our study. Some previous studies also showed that infiltration of $CD8^+$ T lymphocytes and antitumor immunity were not obvious in 4T1 tumors after radiation (3 × 8 Gy).[44,45] These studies indicated that the mechanisms of IR-induced antitumor immunity were complicated and that the dose and dose fraction mode were not the only determining factors in addition to the GSDME level. Additionally, the upregulated levels of GSDME transcription and translation observed in MCF-7 and MDA-MB-231 cells indicate that IR can enhance GSDME expression in some cancer cells. We hope that the underlying mechanism explored in the future can provide significant clinical guidance for cancer therapy.

Mitochondrial (Caspase 9/Caspase 3) or death receptor apoptotic (Caspase 8/Caspase 3) pathways are involved in apoptosis and pyroptosis induction in response to oxidative stress.[46,47] Caspase 3-mediated GSDME cleavage contributes to the switch from apoptosis to pyroptosis.[7] Consistent with a previous study,[12] our findings confirmed that activation of the Caspase 9/Caspase 3/GSDME pathway after IR led to pyroptosis in tumor cells and that GSDME was indispensable in IR-induced pyroptosis. Furthermore, we also observed the cleavage of both PARP and GSDME in GSDME-overexpressing tumor cells, implying the coexistence of apoptosis and pyroptosis after IR in the same cell population, possibly due to the heterogeneity of tumor cells.

Conclusion

We found that IR-induced pyroptosis in tumor cells promoted $CD8^+$ T-cell tumor infiltration to activate the antitumor response. Furthermore, we confirmed that a large fraction of IR was better than conventional IR in triggering tumor cell pyroptosis, and the combination of IR and demethylated drugs or some chemotherapeutic drugs could also induce more extensive pyroptosis than IR alone. Our findings provide a new strategy for clinical RT and theoretical guidance for further optimization of clinical RT plans.

References

1. Nagata S, Tanaka M. Programmed cell death and the immune system. *Nat Rev Immunol* 2017;17:333–340.
2. Snyder AG, Oberst A. The antisocial network: Cross talk between cell death programs in host defense. *Annu Rev Immunol* 2021;39:77–101.
3. Aaes TL, Kaczmarek A, Delvaeye T, et al. Vaccination with necroptotic cancer cells induces efficient anti-tumor immunity. *Cell Rep* 2016;15:274–287.
4. Yu P, Zhang X, Liu N, et al. Pyroptosis: Mechanisms and diseases. *Signal Transduct Target Ther* 2021;6:128.
5. Broz P, Pelegrin P, Shao F. The gasdermins, a protein family executing cell death and inflammation. *Nat Rev Immunol* 2020;20:143–157.
6. Shi JJ, Gao WQ, Shao F. Pyroptosis: Gasdermin-mediated programmed necrotic cell death. *Trends Biochem Sci* 2017;42:245–254.
7. Wang YP, Gao WQ, Shi XY, et al. Chemotherapy drugs induce pyroptosis through caspase-3 cleavage of a gasdermin. *Nature* 2017;547:99–103.
8. Yang XR, Chen GD, Yu KN, et al. Cold atmospheric plasma induces GSDME-dependent pyroptotic signaling pathway via ROS generation in tumor cells. *Cell Death Dis* 2020;11:295.
9. Zhao PF, Wang M, Chen M, et al. Programming cell pyroptosis with biomimetic nanoparticles for solid tumor immunotherapy. *Biomaterials* 2020;254:120142.
10. Liu YY, Fang YL, Chen XF, et al. Gasdermin E-mediated target cell pyroptosis by CAR T cells triggers cytokine release syndrome. *Sci Immunol* 2020;5:eaax7969.
11. Zhang CC, Li CG, Wang YF, et al. Chemotherapeutic paclitaxel and cisplatin differentially induce pyroptosis in A549 lung cancer cells via caspase-3/GSDME activation. *Apoptosis* 2019;24:312–325.
12. Yu JH, Li S, Qi J, et al. Cleavage of GSDME by caspase-3 determines lobaplatin-induced pyroptosis in colon cancer cells. *Cell Death Dis* 2019;10:193.
13. Zhang ZB, Zhang Y, Xia SY, et al. Gasdermin E suppresses tumour growth by activating anti-tumour immunity. *Nature* 2020;579:415–420.
14. Schreiber RD, Old LJ, Smyth MJ. Cancer immunoediting: Integrating immunity's roles in cancer suppression and promotion. *Science* 2011;331:1565–1570.
15. Vanpouille Box C, Pilones KA, Wennerberg E, et al. In situ vaccination by radiotherapy to improve responses to anti-CTLA-4 treatment. *Vaccine* 2015;33:7415–7422.
16. Asano K, Nabeyama A, Miyake Y, et al. CD169-positive macrophages dominate antitumor immunity by crosspresenting dead cell-associated antigens. *Immunity* 2011;34:85–95.
17. Liao Y, Liu S, Fu S, et al. HMGB1 in radiotherapy: A two headed signal regulating tumor radiosensitivity and immunity. *Onco Targets Ther* 2020;13:6859–6871.
18. Park B, Yee C, Lee KM. The effect of radiation on the immune response to cancers. *Int J Mol Sci* 2014;15:927–943.
19. Zhou ZW, He HB, Wang K, et al. Granzyme A from cytotoxic lymphocytes cleaves GSDMB to trigger pyroptosis in target cells. *Science* 2020;368:eaaz7548.
20. Zhang Z, Meng Y, Guo Y, et al. Rehmannia glutinosa polysaccharide induces maturation of murine bone marrow derived Dendritic cells (BMDCs). *Int J Biol Macromol* 2013;54:136–143.

21. Ibrahim J, de Beeck KO, Fransen E, et al. Methylation analysis of Gasdermin E shows great promise as a biomarker for colorectal cancer. *Cancer Med* 2019;8:2133–2145.
22. Luo N, Nixon MJ, Gonzalez-Ericsson PI, et al. DNA methyltransferase inhibition upregulates MHC-I to potentiate cytotoxic t lymphocyte responses in breast cancer. *Nat Commun* 2018;9:248.
23. Tang T, Cheng X, Truong B, et al. Molecular basis and therapeutic implications of CD40/CD40L immune checkpoint. *Pharmacol Ther* 2021;219:107709.
24. Yamauchi T, Hoki T, Oba T, et al. CD40 and CD80/86 signaling in cDC1s mediate effective neoantigen vaccination and generation of antigen-specific CX3CR1^{+}CD8^{+} T cells. *Cancer Immunol Immunother* 2022;71:137–151.
25. Ko EC, Formenti SC. Radiation therapy to enhance tumor immunotherapy: A novel application for an established modality. *Int J Radiat Biol* 2019;95:936–939.
26. Grassberger C, Ellsworth SG, Wilks MQ, et al. Assessing the interactions between radiotherapy and antitumour immunity. *Nat Rev Clin Oncol* 2019;16:729–745.
27. Peng ZYF, Wang PF, Song W, et al. GSDME enhances Cisplatin sensitivity to regress non-small cell lung carcinoma by mediating pyroptosis to trigger antitumor immunocyte infiltration. *Signal Transduct Target Ther* 2020;5:159.
28. Erkes DA, Cai W, Sanchez IM, et al. Mutant BARF and MEK inhibitors regulate the tumor immune microenvironment via pyroptosis. *Cancer Discov* 2020;10:254–269.
29. Tan G, Lin C, Huang C, et al. Radiosensitivity of colorectal cancer and radiation-induced gut damages are regulated by gasdermin E. *Cancer Lett* 2022;529:1–10.
30. Kim MS, Lebron C, Nagpal JK, et al. Methylation of the DFNA5 increases risk of lymph node metastasis in human breast cancer. *Biochem Bioph Res Commun* 2008;370:38–43.
31. Liu YT, Sun ZJ. Turning cold tumors into hot tumors by improving T-cell infiltration. *Theranostics* 2021;11:5365–5386.
32. Son CH, Lee HR, Koh EK, et al. Combination treatment with decitabine and ionizing radiation enhances tumor cells susceptibility of T cells. *Sci Rep* 2016;6:32470.
33. Golden EB, Frances D, Pellicciotta I, et al. Radiation fosters dose-dependent and chemotherapy-induced immunogenic cell death. *Oncoimmunology* 2014;3:e28518.
34. Yoneda K, Kuwata T, Kanayama M, et al. Alteration in tumoural PD-L1 expression and stromal CD8-positive tumour-infiltrating lymphocytes after concurrent chemo-radiotherapy for non-small cell lung cancer. *Brit J Cancer* 2019;121:490–496.
35. Ogura A, Akiyoshi T, Yamamoto N, et al. Pattern of programmed cell death-ligand 1 expression and CD8-positive T-cell infiltration before and after chemoradiotherapy in rectal cancer. *Eur J Cancer* 2018;91:11–20.
36. Zhang Y, Gao J, Wang X, et al. CXCL4 mediates tumor regrowth after chemotherapy by suppression of antitumor immunity. *Cancer Biol Ther* 2015;16:1775–1783.
37. Samanta D, Park Y, Ni X, et al. Chemotherapy induces enrichment of CD47^{+}/CD73^{+}/PDL1^{+} immune evasive triple-negative breast cancer cells. *P Natl Acad Sci USA* 2018;115:E1239–E1248.
38. Zhu X, Cao Y, Liu W, et al. Stereotactic body radiotherapy plus pembrolizumab and trametinib versus stereotactic body radiotherapy plus gemcitabine for locally recurrent pancreatic cancer after surgical resection: An open-label, randomised, controlled, phase 2 trial. *Lancet Oncol* 2021;22:1093–1102.
39. Zhang H, Orme JJ, Abraha F, et al. Phase II evaluation of stereotactic ablative radiotherapy (SABR) and immunity in ^{11}c-choline-PET/CT-identified oligometastatic castration-resistant prostate cancer. *Clin Cancer Res* 2021;27:6376–6383.
40. Evans JD, Morris LK, Zhang H, et al. Prospective immunophenotyping of CD8^{+} T cells and associated clinical outcomes of patients with oligometastatic prostate cancer treated with metastasis-directed SBRT. *Int J Radiat Oncol Biol Phys* 2019;103:229–240.
41. Huang ZZ, Xu Y, Xu M, et al. Artesunate alleviates imiquimod-induced psoriasis-like dermatitis in balb/c mice. *Int Immunopharmacol* 2019;75:105817.
42. Vanpouille-Box C, Alard A, Aryankalayil MJ, et al. DNA exonuclease Trex1 regulates radiotherapy-induced tumour immunogenicity. *Nat Commun* 2017;8:15618.
43. Chang WI, Han MG, Kang MH, et al. PI3K$\alpha\delta$ inhibitor combined with radiation enhances the antitumor immune effect of anti-PD1 in a syngeneic murine triple-negative breast cancer model. *Int J Radiat Oncol Biol Phys* 2021;110:845–858.
44. Zhao Y, Zhang T, Wang Y, et al. ICAM-1 orchestrates the abscopal effect of tumor radiotherapy. *Proc Natl Acad Sci USA* 2021;118:14.
45. Rodriguez Ruiz ME, Rodriguez I, Garasa S, et al. Abscopal effects of radiotherapy are enhanced by combined immunostimulatory mAbs and are dependent on CD8 T cells and crosspriming. *Cancer Res* 2016;76:5994–6005.
46. Broz P. Immunology: Caspase target drives pyroptosis. *Nature* 2015;526:642–643.
47. Boice A, Bouchier Hayes L. Targeting apoptotic caspases in cancer. *Biochim Biophys Acta Mol Cell Res* 2020;1867:118688.